Journal of Infectious Diseases & Therapy
ISSN: 2332-0877

Research Article Open Access

Terminal Restriction Fragment Length Polymorphism Analysis of Bacterial Population Differences in *Mus Musculus* Cecum in Response to Probiotic Administration

Leasha M. Christensen[1], Cynthia Blanton[2] and Peter P. Sheridan[1*]

[1]*Department of Biological Sciences, Idaho State University, Pocatello, Idaho, USA*
[2]*Department of Dietetics, Idaho State University, Pocatello, Idaho, USA*

Abstract

The cecum aids in maintaining homeostasis and host health by having the highest metabolite absorption and housing the most abundant population of microbes in the mouse gastrointestinal tract. Various disease states, for which there is no standard medical treatment, result from the disruption of the microbial populations in either presence or relative abundance due to various environmental and host factors. Supplementation with probiotics, prebiotics, and synbiotics has shown promise as a therapeutic intervention to combat dysbiosis. High throughput, culture-independent 16S rRNA terminal restriction length polymorphism analysis of cecum samples from mice fed a control or synbiotic diet showed conservation of homeostatic balance in synbiotic-supplemented samples according to Shannon, Simpson, and Margalef indices and insights into possible phylogenetics when further processed by Additive Main Effects and Multiplicative Interactions analysis. Additional research is needed to more directly determine the diversity and phylogenetic effects of synbiotic supplementation on cecum content for the alleviation of dysbiosis among the present microbial populations.

Keywords: Dysbiosis; Prebiotic; Probiotic; Synbiotic; T-RFLP; Microbial diversity; AMMI

Introduction

AUnique microbial communities are found within and on humans and other vertebrates, where they colonize diverse environments such as the skin, mucosal surfaces, and the gastrointestinal tract, with the most densely populated region being the large intestine [1-4]. Many of these microbes, which provide the host with metabolic and genetic features that are not innate and therefore develop a synbiotic relationship with the host, reside within the confines of the intestine and are collectively referred to as the "human gut microbiota" or the "gut microbiota, and this microbial assemblage is often referred to in the literature as being a bodily organ [5,6].

Host health is impacted by the microbiota existing within the gastrointestinal tract in that it affects various physiological factors such as: resistance to pathogen colonization, immune response regulation, nutrition, metabolism, development, and host homeostasis [4,7-10]. Being co-evolved, these interactions can be detrimentally affected due to administration of antibiotics and alterations of chemical transformations within the gut and may lead to acute and/or chronic illnesses including: digestive, bowel, eating and weight disorders; cancer; cardiac events; allergies and asthma; type 2 diabetes; atopic diseases relating to the change in microbial community composition; and neurodevelopmental disorders [4,11-23]. The gut microbiota also moderates the programing and control of various physiological functions such as epithelial development and blood circulation, as well as innate and adaptive mechanisms of immunity and energy homeostasis regulation. Therefore, in response to environmental factors that disrupt the host-gut interactions, metabolic diseases may ensue. Various aspects of the 'modern lifestyle' including traveling, dietary changes and restrictions, use of medications, age, urbanization, geographic location, and stress level can disrupt his essential host-microbe interaction [4-6,13,15-17,19,24-34].

Although there is no standard medical treatment, various methods such as fecal-oral transplantations, bacteriotherapy, and antibiotic administration have been employed to treat severe alterations in gut microbial populations upon the development of a disease to a chronic state [5-7,19,24,35-37]. The lack of treatment options usually results in antibiotic administration, which is often unsuccessful. For instance, 20% of patients suffering from a Clostridium Difficile Infection (CDI) have a recurrent episode after initial antibiotic treatment, and patients having a recurrent episode are 40% more likely to experience another [36]. Also, metabolomics studies of 2000 murine metabolite features in fecal samples have shown that a single high dose of streptomycin can cause significant changes in roughly 90% of the features analyzed [33]. The use of fecal-oral transplantations is a highly invasive process including various donor and recipient screenings for compatibility amongst other factors despite potential use [13,24,37]. In light of this the use of probiotics, prebiotics and the combined use as synbiotics as a treatment method shows potential [5,6,16-20,23,25-33,38-40].

Probiotics are "organisms and substances which contribute to intestinal microbial balance" or "a live microbial feed supplement which beneficially affects the host animal by improving its intestinal microbial balance" [24]. In order to fit this definition, which does not include antibiotics, the probiotic needs to be stable and viable and remain as such under storage and during use, survive the intestinal ecosystem, be producible on a large scale, and beneficially affect the host after its administration. Surviving the acidic environment within the gut and then colonizing and becoming active in the colon can be problematic as adherence to the intestinal epithelium may be necessary to insure proteins remain intact and active. Competition for nutrients and ecological niches can also cause a decrease in effectiveness in this treatment. Additionally, the probiotic must also remain present after the consumption of the product initially containing the strain has ended [5,14,15,33,41]. *Lactobacilli, Bifidobacteria*, and *Streptococci* are commonly used in probiotic treatments and have been shown to alleviate

***Corresponding author:** Peter P. Sheridan, Department of Biological Sciences, Idaho State University, Pocatello, Idaho, USA, E-mail: sherpete@isu.edu

Received date: April 07, 2020; **Accepted date:** April 21, 2020; **Published date:** April 30, 2020

Citation: Bernadette AK, Artemio R (2020) Dengue Cerebellitis in An Adult Male - A Case Report & Literature Review. J Infect Dis Ther S4: 001.

hepatic encephalopathy, carcinogenesis, diarrhea, colitis, pathogen colonization, constipation, gastroenteritis, immunostimulation, flatulence, and gastric acidity among other diseased states [15,33,41]. *L. acidophilus* is the most commonly used and tolerated probiotic and has been shown to synthesize vitamin K, which is necessary for the conversion of the bone matrix osteocalcin to the active form and may thus aid in improving bone integrity [5,14-17,26-33,38,39,41,42].

Prebiotics are defined as being "a non-digestible food ingredient that beneficially affects the host by selectively stimulating the growth and/or activity of one or a limited number of bacteria in the colon, and thus improves host health" [24]. Prebiotics must serve selectively as a substrate for specific commensal, beneficial bacteria for growth or metabolic activation while not being absorbed or hydrolyzed prior to reaching its final destination. Its application must also result in microbial composition alterations to achieve a state of health while also providing systemic or luminal effects that benefit host health [5,14,33]. Non-digestible foods, or prebiotics, such as oligosaccharides, polysaccharides, fructooligosaccharidesnd other naturally occurring non-digestible carbohydrates (resistant starch, nonstarch polysaccharides [hemicellulose, pectins, gums, plant cell wall polysaccharides]), peptides, and lipids have been shown to improve host gut microbiota health by stimulating growth and activity of specific endogenous microbiota by changing the microbial composition of the local environment. Lack of absorption and digestion of these compounds is due to their chemical structure [33,43]. These compounds have been shown to particularly benefit host colonic health, and can directly manipulate metabolism of lipids via products of fermentation.

The combined use of probiotics and prebiotics is referred to as synbiotics, or "a mixture of probiotics and prebiotics that beneficially affects the host by improving the survival and implantation of live microbial dietary supplements in the gastrointestinal tract, by selectively stimulating the growth and/or by activating the metabolism of one or a limited number of health-promoting bacteria, and thus improving host welfare" [24]. They have shown promise in combating the diseased dysbiosis state and can also increase the viability and functional activity of exogenous and endogenous bacteria. Synbiotics may also prove useful in combatting pathogenic bacterial overgrowth, parasite growth, viral infections, the negative effects of burn treatment, stress, and antibiotic therapy effects as these are associated with the translocation of bacteria due to the failure of the intestinal barrier [5,14,15,33].

Due to the lack of information pertaining to the composition of the gut microbiota under both healthy and diseased states, supplementation of effective pre- and probiotics has been challenging. Species shifts between the two states of health have remained elusive despite the current knowledge of phyla level changes. This current lack of information further limits the understanding of microbial community interactions on the supplemented treatments due to the heterogeneity of bacterial spatial distribution within the GI tract according to environmental differences. This results in differing activities of the components of synbiotics across different microbiotic communities along the gastrointestinal tract. Within a local environment, the metabolic products of one bacterial species can be modified and utilized by another bacterial species, so increasing the availability of a molecule in its active form can be affected by community level biotransformation reactions. These cooperative interactions directly affect the degree of effectiveness of a prebiotic, as the necessary active form may never reach its target location, or a probiotic, which may contain a strain that does not yield the desired, beneficial effect on microbial composition and function. Further research is needed to investigate and characterize the intestinal communities of microbes to increase the efficiency and effectiveness of synbiotic treatments [15,33].

Many gastrointestinal tract microbes cannot be isolated and cultured by traditional culture-dependent techniques, making characterization of complex microbial community samples an arduous process that limits many microbial ecology studies due to the difficulties of identification and quantification of microorganisms present within any given sample. Culture-dependent methods are restricted due to the limited information available from morphological data and the difficulties of isolation. As such, diversity can be more adequately assessed¬¬¬¬¬ by molecularly-based techniques due to their applicability to a wide range of organisms [44]. Various initiatives in both the US and Europe have been employed to increase the knowledge base through characterization of the microbes and their genomes within the human body for assessment of their impact and role in states of health and disease (Human Microbiome Project and MetaHIT Consortium, respectively) [5,6,15,33]. Although progress has been made, the gut microbiome has yet to be characterized in its entirety. The intestinal microbial community is composed primarily of bacteria, weighs more than 1.5 kg in humans, and includes over 1100 species [5,6,15,33]. There is something in the range of 1011-1014 bacteria per gram of intestinal material, and characterization of this community requires a high-throughput means of DNA analysis due to the lack of accurate representation of diversity from culture-dependent methods of analyses [15].

Terminal Restriction Length Polymorphism (TRFLP) is ideal for utilization as a cultural-independent means of rapid, high throughput, robust and quantitative analysis (statistical as well as molecularly) of the microbial community composition, diversity, and structure present within the mouse cecum tissue culture by means of fluorescent dyes that attach to PCR primers and the resolution achievable in current sequencing technologies [45-48]. Analysis of the data is also greatly facilitated through the use of current, improved fragment and sequence analysis and software packages allowing for statistical precision and a higher degree of resolution between data samples yielding a clearer, more accurate representation of biological patterns and increased application in microbial community dynamics on a scale previously unobtainable [44,47,49]. It has been successfully utilized in bacterial community differentiation amongst a wide variety of sample sources. In addition to community differentiation, it can also be applied to analysis of the relative structure and phylotype richness of a community as well as to relative organism identification, thus bypassing the limitations present in cultivation-dependent methods. It can also confidently have application in community structure analysis of spatial and temporal shifts. The use of 16S rRNA amplicons in the production of TRFLP patterns also has applications related to diversity studies of the community profile by providing insights pertaining to the detection of rare phylotypes as well as past-unexplored biodiversity and ecological characteristics of either individual taxa or whole microbial communities. Additionally, the TRFLP patterns are generated by electrophoretic systems integrated into DNA sequencing platforms, thus enabling greater precision and higher resolution that any other current community profiling method available [47,48,50-52].

The simplest approach to trace analysis is a binary comparison of sample peak presence. Although valid, this approach lacks appropriate quantitative analysis. ANOVA, which provides a description of the main effects and quantification of interactions through analysis of variance, allows analysis of this as well as establishing whether either factor influences the microbial composition on an individual basis or may result from a contribution interaction among factors present

[53-55]. It is integrated in Additive Main Effects and Multiplicative Interactions (AMMI) analysis to separate variation into interactions and main effects (TRFLP and environmental, or E, variation) and then it later applies PCA to the interactions to create Interaction Principal Components (IPCs), thus focusing on the effects of treatments and environments on resulting TRFLPs [34]. Relative stability conclusions, in addition to identification of genotype assignments to given locations while simultaneously summarizing interaction and main effects, can be elucidated by biplots and is most successful when the genome-environmental interaction is concentrated most heavily in the first or the first two PCA axes as the use of more than two does not contribute to observations or validate results since noise is predominantly captured in subsequent PCAs [34,53,54]. When equally studying main effects and interaction, employment of the AMMI model can increase accuracy by incorporating both ANOVA and PCA into a single methodology. Within the AMMI model, ANOVA analysis separates interaction from the additive component of the data to which PCA is then applied as a multiplicative model for analysis of the interaction generated from the additive ANOVA. Both biotic and abiotic stressors can be correlated with genotype to environmental interactions [54]. PCA and other multivariate statistical methods have been used to employ the needed statistical rigor for complex data set analysis. An additional benefit to multivariate analyses is the use of numerous variables that are not constrained to species identification. PCA can be used to show trends in distances in community patterns. However, PCA data is not normally distributed. Additionally, non-linear data from large gradients can cause PCA ordination arcing and thus obscure any patterns, yet AMMI has increased utility as it can be applied to interactions that are non-linear in a complex model while discarding noise and also aids in variation measures within a dataset including IPC interaction signals [34,53,56].

Mouse models allow for increased control during analysis as well as a decrease in the number of confounding variables while providing representation to the human microbiome, and beta diversity results showed that there was no significant difference in the generated means [16,57,58]. Diversity studies are imperative to analysis of community structure and function, especially in relation to development of pharmaceuticals, probiotics, bioaugmentation, or substrate presence [32]. In order to determine measurable microbial diversity baselines and shifts in diversity and frequency of bacterial lineages in mouse cecum samples upon the administration of pre- and probiotics, we performed an intensive study of microbial flora in response to the administration of different probiotic diets due to the high metabolite absorption rate within the cecum [3,5,6,19,20,22,25-32,41,59].

Methods

Sample preparation

Three samples each of harvested cecum from male 9-mo-old mice (Harlan), *Mus musculus*, following either a controlled (B, C, F) or synthetic (H, J, L) diet were chosen at random. Based on a powdered form of American Institute of Nutrition (AIN)-93M purified rat diet (Dyets, Inc., Bethlehem, PA), the diets were modified to utilize cornstarch in place of sucrose and dextrin in order to reduce the susceptibility of osmotic dehydration of the bacteria studied within the synthetic diet. The isocaloric diets administered were composed based on carbohydrate ingredient manipulation by "assuming energy densities of 4, 0, and 2 kcal/g for cornstarch, cellulose, and fructooligosaccharide, respectively [60]." Nutraceutix, Redmond, WA, provided fructooligosaccharide and lyophilized probiotic cultures (1 × 1011 CFU/g of equal parts Lactobacillus acidophilus and Lactococcus lactis lactis). The diets were made fresh three times a week with addition of probiotics immediately prior to feeding each morning for 18 weeks [60].

The harvested diet-specific cecum samples were then sterilely dissected both laterally and vertically, and rehydrated using 6 mL of 10 mM TRIS, pH ~ 8.0, 1% Triton after being stored at -20˚C. Samples were then incubated at 80˚C for one hour, and large debris and mouse tissue was removed by a low-speed spin (1000 rpm) for five minutes. The supernatant containing bacteria was centrifuged at 16,000 xg for 10 minutes to produce a gut microbiota cell pellet. The cell pellet was resuspended by addition of 250 uL 10 mM TRIS.

DNA isolation

Genomic DNA of the cecum samples was obtained by a mechanical sheer forces protocol utilizing 100 µL Lysozyme (100 mg/mL) added to the rehydrated cell suspension solution and incubation for 30 minutes at 37˚C. After which, 100 µL Proteinase K (10 mg/mL in 10 mM TRIS) was added, incubated for 30 minutes, and brought up to 1.8 mL with Lysis buffer (500 mM NaCl, 50 mM ETDA, 1% SDS [w/v], and 50 mM TRIS (pH 8.0) in a bead-beating tube. Tubes were then bead-beated for 5 minutes, boiled at 80ºC for 10 min, and microcentrifuged at 3000xG for 5 minutes. Supernatant (750 µL) was added to 450 µL of 100% isopropanol and stored at -20˚C for 12 hours. Samples were then centrifuged at 13000 xG for 10 min, and the pellet washed with 200 µL 70% ethanol (4˚C) prior to centrifugation at 13000 xG for 10 minutes. Ethanol was removed via pipetting, followed by drying at 37˚C for 60 minutes before DNA was rehydrated in 100 µL 10 mm TRIS, pH ~ 8.0.

T-RFLP and PCR amplification

A bacterial SSU rDNA T-RFLP polymerase amplification with the fluorescently-tagged universal bacterial 1492R (5'-FAM/TTACCTTGTTACGACTT-3') and 8F (5'HEX/AGAGTTTGATCCTGGGCTCAG-3') primers (1 mm) and 1U (0.5 µL) Vent exo (-) (New England Biolabs, Ipswich, MA) was performed in triplicate in 50 µl reactions for each of the genomic DNA samples with each reaction containing the following: 1 X ThermoPol Buffer (New England Biolabs, Ipsich, MA), 400 µm of each deoxynucleotide triphosphate (New England Biolabs, Ipswich, MA), and 1 µL 20 µM genomic DNA template. Individual master mixes and negative controls were used for each sample in a program consisting of the following steps: 10 minute denaturation at 95˚C, followed by 30 cycles of 95˚C for 1 minute, 52. ˚C for 2 minutes, and 4 minutes at 72˚C, with the final cycle followed by a 10 minute elongation step at 72˚C. After visualization via low EEO 1% agarose gel stained with ethidium bromide, the TRFLP PCR products were purified using a Gene JET PCR Purification kit (Thermo Scientific).

10 uL of the purified TRFLP amplicons were digested with 5 U (0.25 uL/reaction) of the restriction endonuclease TaaI (Thermo Scientific), in 20 uL 10 X Tango buffer and 18.75 uL nuclease-free water at 65˚C for 2 hours. The TRFLP digests were then purified by precipitating the fragments with 5 µL 3 M sodium acetate and 100 µL 70%, and resuspending the pellet in 10 uL nuclease-free water. 1 µL purified terminal restriction fragments (TRFs) were then submitted to the Idaho State University Molecular Core Facility for size determination utilizing a GeneScan™ 1000 ROX™ Size Standard (Applied Biosystems) for fluorescently labeled DNA on a 3130 XL Genetic Analyzer (Applied Biosystems, Foster City, CA).

Statistical and data analysis

Raw terminal restriction fragment size and peak area data generated for each sample was analyzed using NPP analysis in Peak

Scanner Software V.1.0 (Applied Biosystems). Fragments exceeding the threshold value (50 RFU) and designated as representative peaks and not noise in comparison to the size standard were analyzed using Primer 6 software (PRIMER-E Ltd, Plymoutoh, United Kingdom) following all default settings with the exception of 'samples set as rows' in order to generate respective statistical diversity indices of Margalef Species Diversity values (species abundance and frequency), Shannon Diversity Index values (entropy or proportional abundance of a given species amongst a whole), and Simpson Index values (probability of two randomly selected 'samples' belonging to the same species) for comparison amongst the diets and individual cecum samples.

AMMI

AMMI analysis investigating microbial community variation and environmental effects on microbial flora within the cecum ecosystem of the mouse intestinal microbiome was performed using TRFLP peak values and the web-based T-REX, or TRFLP analysis expedited) (http://trex.biohpc.org/) program [57]. A clustering threshold of 0.5 was selected in addition to analysis according to peak height. All other default settings were utilized. An Analysis of Variance (ANOVA) was generated and interaction principal component analysis (IPCA) was then performed on the resulting ANOVA data through use of the same software to reduce the dimensionality of the multivariate data. This analysis allowed for the visualization of the main effects and interactions of microbial environment and genotypes simultaneously, and IPCA values corresponding to primary and secondary axes were then graphed (Microsoft Excel) for the generation of representative peak variability in relation to the 5' and 3' T-RFLP fragments. Analysis was performed in nine ways: individual analyses was performed on the control diet of each the forward and reverse primer and then both primers together; this was then replicated for the synthetic diet and for both diets together.

Results

Control

The control forward fragment TFR profile depicted the two-dimensional interactions and variations produced by analyzing the forward HEX fragment of the control diet fed mice (B, H, J) (Figure 1). 74.09% variation was produced within the analysis. This data produced a mean square error rate of 0.03571, 36.32% TRF main effects percent variation total, interaction percent variation total composed of 50.6% pattern and 13.08% noise, and an 88.96825 total sum of squares value (data not shown).The analysis of the reverse fragment of the control diet analysis represented 285.15% measured variation amongst the replicates of these samples (Figure 2).

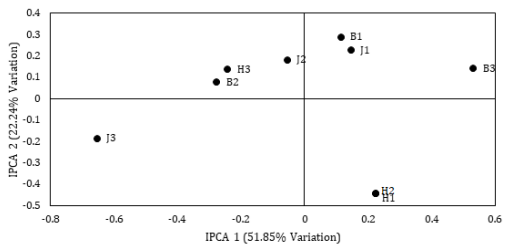

Figure 1: 16S bacterial amplicon T-RFLP analysis from the molecular-based microbial community fingerprinting technique, T-REX (T-RFLP analysis Expedited), on the forward 5' HEX fragment of triplicate mouse cecum samples harvested from the cecum content of control (B, H, J represented by closed circles) diet fed mice. The letter for each data point represents the sample and the following the number the replicate number. Stacked point designations represent data having the save value and coordinate.

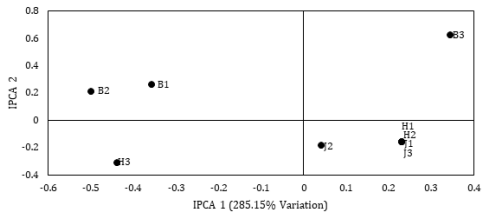

Figure 2: 16S bacterial amplicon T-RFLP analysis on triplicate mouse cecum samples harvested from the cecum content of control (B, H, J represented by closed circles) diet fed mice where the letter represents the sample and number the replicate. Data is presented by means of the AMMI model, which organizes variations and interactions amongst data by means of ANOVA and PCA. The figure above depicts the reverse 3 FAM fragments yielded by T-REX of the control mice. Stacked point designations represent data having the same value and coordinate.

These data produced a mean square error rate of 0.10741, 48.78%TRF main effects percent variation total, interaction percent variation total composed of 8.81% pattern and 42.41% noise, and a 30.70833 total sum of squares value (data not shown). 69.39% variation of the sample replicates was represented in two-dimensional analysis (Figure 3). These data produced a mean square error rate of 0.02673, 21.05% TRF main effects percent variation total, interaction percent variation total composed of 65.78% pattern and 13.17% noise, and a 168.69399 total sum of squares value (data not shown).

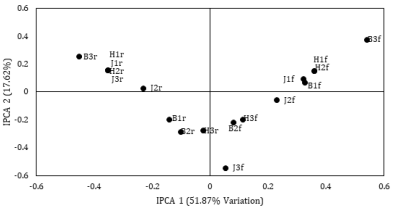

Figure 3: 16S bacterial amplicon T-RFLP analysis on triplicate mouse cecum samples harvested from the cecum content of control (B, H, J represented by closed circles) diet fed mice. Data is presented by means of the AMMI model, which organizes variations and interactions amongst data by means of ANOVA and PCA. The figure above depicts the forward 5' forward HEX and reverse 3' FAM fragments yielded by T-REX of the control mice. Each sample has triplicate forward and reverse data points. The number after the initial sample letter designation depicts the replicate number and the concluding f or r forward and reverse, respectively. Stacked point designations represent data having the same value and coordinate.

Synbiotic

The two-dimensional analysis of the synbiotic forward fragment captured a total of 59.56% variation (Figure 4). This data produced a 26.57%TRF main effects percent variation total, a 70.58% interaction percent variation total, and 42043682.93 total sums of squares (data not shown).

Data corresponding to the reverse 3' FAM fragments yielded by T-REX analysis of the synbiotic mice is shown in Figure 5. A total of 89.92% is captured by both IPCA 1 and 2 values. This data produced 42.27% TRF main effects percent variation total, 42.27% interaction percent variation total, and a 4715170.35069 total sum of squares value (data not shown). A 54.63% total variation was captured from analysis of IPCA 1 and 2 of the forward and reverse TRF profiles of synbiotic mice (Figure 6). This data produced a 12.77% TRF and 3.72% environmental main effects percent variation total, 83.52% interaction percent variation total, and 51663738.15435 total sums of squares (data not shown).

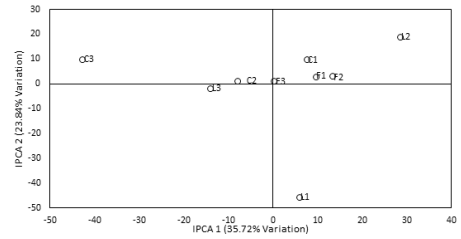

Figure 4: 16S bacterial amplicon T-RFLP analysis on triplicate mouse cecum samples harvested from the cecum content of synbiotic (C, F, L) diet fed mice where the letter represents the sample and number the replicate. Data is presented by means of the AMMI model, which organizes variations and interactions amongst data by means of ANOVA and PCA. The figure above depicts the forward 5' HEX fragments yielded by T-REX analysis of the synbiotic mice which are designated as open circles.

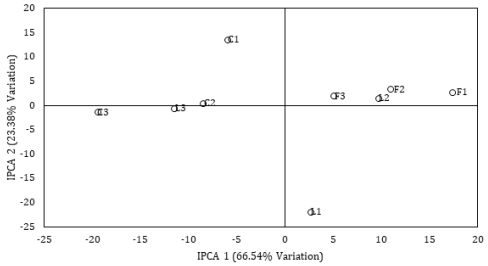

Figure 5: 16S bacterial amplicon T-RFLP analysis on triplicate mouse cecum samples harvested from the cecum content of synbiotic (C, F, L designated as open circles) diet fed mice of the reverse 3' FAM fragment where the letter of each data point corresponds to the sample and number the replicate. Data is presented by means of the AMMI model, which organizes variations and interactions amongst data by means of ANOVA and PCA.

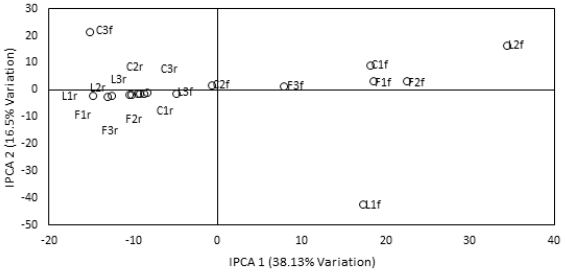

Figure 6: 16S bacterial amplicon T-RFLP analysis on triplicate mouse cecum samples harvested from the cecum content of synbiotic (C, F, L which are designated as open circles) diet fed mice. Data is presented according to AMMI analysis. The figure above depicts the forward 5' HEX and reverse 3' FAM fragments yielded by T-REX analysis of the synbiotic mice. Each sample has triplicate forward and reverse data points. The numbers after the initial sample letter designation depicts the replicate number and the concluding f or r forward and reverse, respectively. Stacked point designations represent data having the same value and coordinate.

Combined diet

The relationship of the forward fragment of both diet samples combined and resulted in a 56.41% variation (Figure 7). Data analysis yielded a mean square error rate of 0.02857, 33.09%TRF main effects percent variation total, interaction percent variation total composed of 54.13% pattern and 12.78% noise, and a 172.21587 total sum of squares value (data not shown).

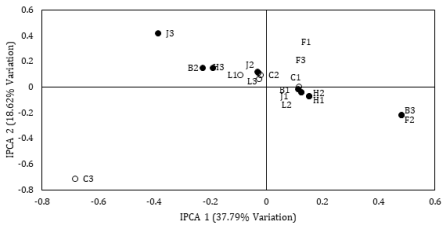

Figure 7: 16S bacterial amplicon T-RFLP analysis on triplicate mouse cecum samples harvested from the cecum content of control (B, H, J designated by closed circles) and synbiotic (C, F, L represented by open circles) diet fed mice. Data is presented by means of the AMMI model, which organizes variations and interactions amongst data by means of ANOVA and PCA. This is a graphic representation of the 5' forward HEX yielded by T-REX of the control and synbiotic mice. Stacked point designations represent data having the same value and coordinate. The letter in the label of each data point corresponds to the sample and the number the replicate.

An IPCA value of 958.57 % in the first axis was generated in when investigating the reverse fragment of the combined analysis of both the control and synbiotic diets (Figure 8). This data analysis yielded a mean square error rate of 0.089027, 58.95% TRF main effects percent variation total, interaction percent variation total composed of 2.1% pattern and 38.94% noise, and a 62.35985 total sum of squares (data not shown). 63.5% variation was produced in the analysis of both the forward and reverse fragments of both diets combined (Figure 9). This data analysis yielded a mean square error rate of 0.02158, 22.77% TRF main effects percent variation total, interaction percent variation total composed of 64.89% pattern and 12.34% noise, and a 341.95604 total sum of squares value (data not shown).

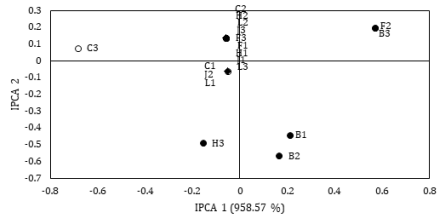

Figure 8: 16S bacterial amplicon T-RFLP analysis on triplicate mouse cecum samples harvested from the cecum content of control (B, H, J represented by a closed circle) and synbiotic (C, F, L designated as an open circle) diet fed mice. Data is presented by means of the AMMI model, which organizes variations and interactions amongst data by means of ANOVA and PCA. The figure above depicts the reverse 3' FAM fragments yielded by T-REX of the control and synbiotic mice. Stacked point designations represent data having the same value and coordinate. Data labels correspond to the sample (letter) and replicate (number).

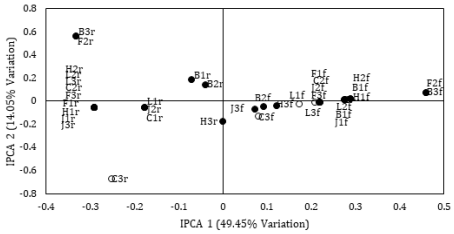

Figure 9: 16S bacterial amplicon T-RFLP analysis on triplicate mouse cecum samples harvested from the cecum content of control (B, H, J represented by a closed circle) and synbiotic (C, F, L designated as an open circle) diet fed mice. Data is presented by means of the AMMI model, which organizes variations and interactions amongst data by means of ANOVA and PCA. The figure above depicts the 5' forward HEX and reverse 3' FAM fragments yielded by T-REX of the control and synbiotic mice. Each sample has triplicate forward and reverse data points. The numbers after the initial sample letter designation depicts the replicate number, and the concluding f or r forward and reverse, respectively. Stacked point designations represent data having the same value and coordinate.

Representative diet samples

Two-dimensional interactions and variations produced by analyzing the forward HEX fragment of the "best" representative control (H) and synbiotic (L) diet as determined by Peak Scanner absorbance plots of TRFLP data and yielded a total of 138.23% variation in regards to both axis (Figure 10). This data analysis yielded a mean square error rate of 0.06667, 40.32%TRF main effects percent variation total, interaction percent variation total composed of 30.79% pattern and 28.9%noise, and a 32.15 total sum of squares value correlating to the diversity among environments and variation (data not shown).

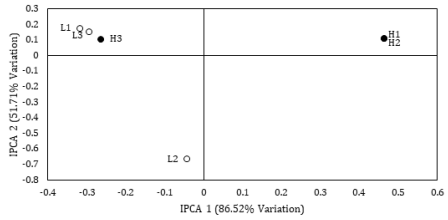

Figure 10: 16S bacterial amplicon T-RFLP analysis from the molecular-based microbial community fingerprinting technique, T-REX (T-RFLP analysis Expedited), on mouse cecum samples harvested from the cecum content of control (H, designated by a closed circle) and synbiotic (L, represented by an open circle) diet fed mice. Data is presented by means of the AMMI model. The figure above depicts the two dimensional interactions and variations produced by analyzing the forward 5' HEX fragment of the "best" representative control (H) and synbiotic (L) diet as determined by Peak Scanner absorbance plots of TRFLP data. Stacked point designations represent data having the same value and coordinate.

The reverse 3'FAM fragments yielded by T-REX of the control (H) and synbiotic (L) mice, where each sample had triplicate forward and reverse data points and the number after the initial sample letter designation, depicted the replicate number yielded a negative 147.7% variation (Figure 11). This data analysis yielded a mean square error rate of 0.14286, 69.51%TRF main effects percent variation total, interaction percent variation total composed of -20.64% pattern (a negative interaction) and 51.14% noise, and an 18.38095 total sum of squares value correlating to the diversity among environments and variation (data not shown).

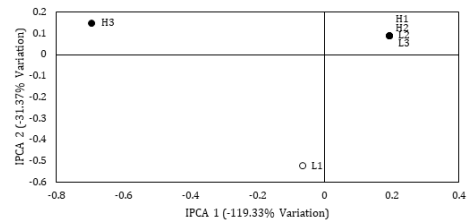

Figure 11: 16S bacterial amplicon T-RFLP analysis on triplicate mouse cecum samples harvested from the cecum content of control (H) and synbiotic (L) diet fed mice. Data is presented by means of the AMMI model, which organizes variations and interactions amongst data by means of ANOVA and PCA. The figure above depicts the reverse 3' FAM fragments yielded by T-REX of the control (H) and synbiotic (L) mice. Each sample has triplicate forward and reverse data points. The number after the initial sample letter designation depicts the replicate number. Stacked point designations represent data having the same value and coordinate.

The 5' forward HEX and reverse 3' FAM fragments yielded by T-REX of the control (H) and synbiotic (L) mice "best" sample designated by data collected by Peak Scanner showed each sample having triplicate forward and reverse data points (Figure 12). The numbers after the initial sample letter designation depicts the replicate number and the concluding f or r, forward and reverse, respectively. Complete variation capture among the first two PCA values yielded a total of 90374.3% variation is represented by both IPCA 1 and 2 with increased variation in IPCA 1. This data analysis yielded a mean square error rate of 0.04545, 24.56% TRF main effects percent variation total, interaction percent variation total composed of 47.54%pattern and 27.89% noise, and a 63.64091 total sum of squares value correlating to the diversity among environments and variation (data not shown).

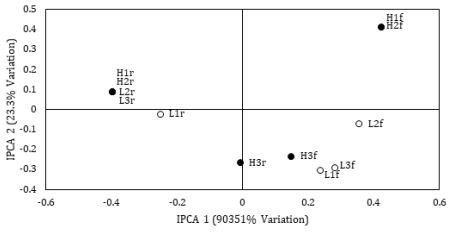

Figure 12: 16S bacterial amplicon T-RFLP analysis on triplicate mouse cecum samples harvested from the cecum content of control (H, closed circle) and synbiotic (L, open circle) diet fed mice. Data is presented by means of the AMMI model, which organizes variations and interactions amongst data by means of ANOVA and PCA. The figure above depicts the 5' forward HEX and reverse 3' FAM fragments yielded by T-REX of the most representative sample of each the control and synbiotic mice. Each sample has triplicate forward and reverse data points. The numbers after the initial sample letter designation depicts the replicate number and the concluding f or r forward and reverse, respectively. Stacked point designations represent data having the same value and coordinate.

Diversity indices

Diversity indices representing the average Margalef species richness (d) of TRF profiles generated by cecum content of control (B, H, J) and synbiotic (C, F, L) diet fed mice is represented in Figure 13; Shannon Diversity (Figure 14); Simpson diversity Index (1-Λ') (Figure 15).

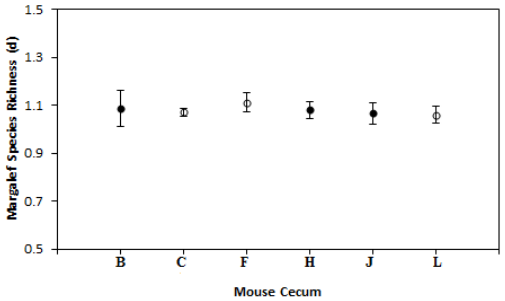

Figure 13: Diversity indices representing the average Margalef species richness (d) values produced by Primer 6 software during terminal restriction fragment length polymorphism analysis comparing cecum content of control (B, H, J designated as closed circles) and synbiotic (C, F, L represented as open circles) diet fed mice. This diversity index measures species abundance and frequency.

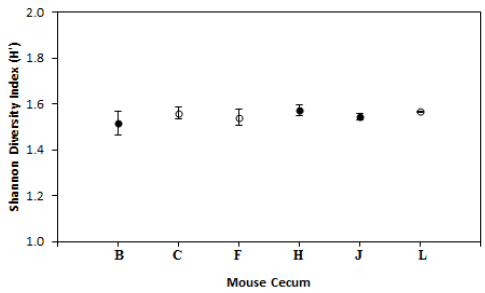

Figure 14: Average Shannon diversity indices (H') values of sample replicates produced by Primer 6 software during T-RFLP analysis of mouse cecum tissue samples harvested from mice fed either a controlled (samples B, H, J designated as closed circles) or synbiotic diet (samples C, F, L represented as open circles). Error bars were generated from obtaining standard deviations of the averaged replicates.

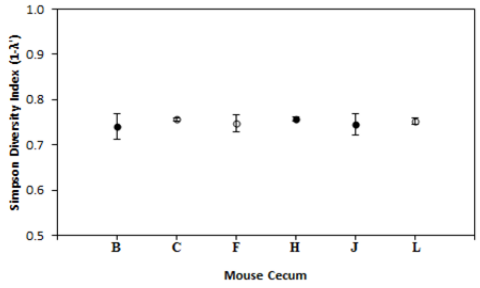

Figure 15: Primer 6 generated average values depicting the probability of two randomly selected samples belonging to the same species, or the Simpson Index (1-λ'), from T-RFLP data of mouse cecum tissue samples collected from mice fed either a controlled (samples B, H, J designated as closed circles) or synbiotic diet (samples C, F, L represented as open circles).

DISSCUSION

A significant total of 74.09% variation was captured in the analysis of the forward fragment of control diet mice thus providing adequate representation of the data (Figure 1). Greater than twice as much variation was generated among the x-axis (IPCA 1) than the y (IPCA 2). The replicates of each of the mice were not all located in proximity of one another and related to increased variation and interaction amongst sample replicates, as shifts in ordination were determined by relative vector distance from the ordinate or other data points present [61]. 66% of the data points are located in quadrants one and two of the figure. High similarity and overlap was evident in respect to mouse H only. Those points having a position less than or close to 0 on the y-axis had a negative correlation or interaction to the other points and were considered more stable due to the relative reduction in interaction effects present on those data points, as the end point of the vector from the origin determines the stability of the genotype in the given environment. Those farther from the origin, as can be determined by vector projection, were more sensitive and adaptable to the environmental parameters applied through the application of the diet. The most ideal genotypic content was found in quadrant 1, as there was a positive interaction in regards of both IPCA 1 and 2. Quadrant 2 represented a low yielding, stable genotype, quadrant 3 an unstable, low- yielding genotype, and 4 an unstable high-yielding genotype. An 88.96825 total sum of squares value correlated to increased diversity among environments and thus the cause of generated variation in this dataset.

Figure 2 produced a high percentage of relative variation among the reverse fragment within the control diet cecum. The cumulative percentage exceeding 100% corresponded to complete capture and complete recovery of all predicted signal. No variation was generated on a two-dimensional basis as there is no variation value represented on the y-axis. Not all replicates shared the same location or were in close proximity within the figure. The exception was found with samples J and H. Replicates 1 and 2 of H and 1 and 3 of J shared the exact position within the fourth quadrant of the graph. This correlated to decreased variation and a high interaction amongst these replicates due to a lack of projected vector shared by each of the data points. The second replicate of J was within the same quadrant as the other two replicates of that sample. The location of data points belonging to all of the replicates of J and the first two replicates of H had a positive interaction due their presence in the same quadrant. Both samples H and B had two replicates within the same quadrant with the remaining replicate in another quadrant. This showed increased, positive interaction between replicates 1 and 2 of each sample independently and decreased interaction with its remaining replicate. Replicates from sample B had positive interactions with the environment due to their location on the y-axis. The scatter of replicates from sample B correlated to variability in both main effects and interactions. Those samples closer to the origin were less adaptive and less sensitive to the environmental influences wrought on by the diet and were more stable. The total sum of squares value from this data set correlated to an overall lack of diversity among environments.

Figure 3 showed an interesting 'mirrored' relationship of the sample replicates in an analysis of the control samples for both forward and reverse fragments. In some cases, one direction (either forward or reverse) of the sample replicate was found in the mirrored opposite relative position of the graph as was seen in B2, B3, H1, H2, and H3. J2 was close to following this pattern. Shared data points, represented by stacked replicates, showed a positive, increased interaction and decreased variation. A total of 69.39% variation of the sample replicates was represented in the two dimensional analysis above. There was more variation in the x-axis than in the y-. Points closer to the origin were less sensitive and were less adaptable to the environmental effects. Those samples with the most ideal genotype were found in quadrant 1.This data produced a mean square error rate of 0.02673, 21.05% TRF main effects percent variation total, interaction percent variation total composed of 65.78% pattern and 13.17% noise, and a 168.69399 total sum of squares value correlating to increased diversity among environments and variation (data not shown). The scatter of data points across the biplot correlated to variability in both main effects and interactions.

There was slightly more variation correlated to the x-axis (IPCA 1) than the y-axis (IPCA 2) within the synbiotic analysis of the forward fragment represented by the listed percent variations on the axis legends (Figure 4). Notably, there was overlap of data points within this analysis. However, there was increased localization of data points amongst the origin which demonstrated increased stability of variety and environment due to the reduced interaction effects. Sample replicates did not share close proximity with the exception of the slight closeness within the F sample replicates. The samples were spread out showing increased variation and less interaction and stability among sample replicates. Increased dimensional analysis could include a higher degree of variation. Replicate L1 was the most unstable as its

vector from the origin is the largest and its overall value was negative relative to its position in quadrant 4. The total sum of squares value resulting from this data set correlated to immense diversity among environments and variation.

A significant percentage of IPCA values were captured in the analysis of reverse fragments within the cecum of synbiotic mice. Increased variation was found in IPCA 1 compared to IPCA 2. Clustering of data points was evident in both quadrant 1 and 2. L1 is the most isolated of all the rest of the data points. Quadrant 1 contained the most replicates. However, 7 of the 9 data points were either on or very near to the origin or have a close to 0 value in terms of IPCA 2 value. Increased variation and diversity among environments related to the sum of squares produced for this data set.

The relatively low percent variation produced from the combination of both HEX and FAM profiles within the symbiotic mice did not contribute to a significant amount of interaction capture within the biplot to be considered fully representative of the dataset (figure 6). More variation was found in IPCA 1 than 2. Ideal genotypes were located in quadrant 1 (5 replicates present). However, many of the replicate data points were located among the origin or across the x-axis. The clustering of data points, when regarded in terms of ordination shifts according to vector distance from the ordinate or from other data points yielded decreased interaction across data within the same general location. L1f had the most negative interaction relative to the rest of the data points. The reverse fragments were more clustered than the forward, and with the exception of l3f, there was separation of the fragments on the graph. The forward fragments were found further from the origin than the reverse. The sum of squares value relative to this data set correlated to increased diversity among environments.

A lack of significant interaction capture to be considered fully representative of the dataset applied to the analysis of the forward fragment of both of the diets combined due to the low percent variation (Figure 7). IPCA 1 had the most variation and increased replicate clustering about its axis. The diets did not separate from one another or follow any distinct patterns. All replicates of a given sample were not found within the same area. Quadrant 1 contained no replicates, and therefore there was no positive interaction or correlation amongst the replicates present. C3 was the largest outlier, having the largest ordinate vector to the origin or other data samples. Some of the replicates (H1 and 2 as well as F1 and 3) shared a location on the graph.

A complete capture in variation was evident in the IPCA value of the reverse fragment analysis of both the control and synbiotic diets (Figure 8). 14 of the 18 replicates shared a data point, or location on the graph. Only 2 of all of the replicates measured were found in quadrant 1. These 2 data points had a positive correlation and variability. The rest of the data points had negative variation. None of the replicates shared the same location for a given sample.

The percent variation value produced from both fragments within the combined diets did not contribute to adequate representation of the sample summary by the analysis provided (Figure 9). There was more variation about the x-axis (IPCA 1) than the y (IPCA 2). Stacked replicate designations showed shared data point position, increased interaction, and decreased variation amongst replicates included. 27 of the data points shared data share the same location with at least one other data point. 14 of the 27 were reverse replicates. Replicate data points having a shared locale interestingly had the same fragment designation, either forward or reverse. There were no shared data points between both of the fragment types. Additionally, each quadrant only contained one fragment designation. The graph was split with forward fragments on the right side (Quadrants 1 and 4) and reverse fragments on the left side (Quadrants 2 and 3). The forward fragments were clustered more around the x-axis than the reverse. Increased proximity correlated to decreased variation and increased interaction between the sample data points.

Of the representative samples from each diet sample set, none of the data points included in this figure of forward fragments were clustered about the origin (Figure 10). However, each representative sample produced two of its three replicates within the same general area. The higher interaction effects were unstable causing the measured variability in the produced means. The closeness, as measured from a projected vector connecting the data points, correlated to decreased variation and increased interaction. Those with a positive correlation to variation were in Quadrants 1 and 2. Quadrant 1, which housed a shared data point for H replicates 1 and 2, had the most positive correlative values. L2 in quadrant 3 had the most negative correlative. Neither sample had all of its replicates clustered about a given data point. There was more variation in IPCA 1 than IPCA2. The relatively small sum of squares for the environments of this dataset coincided with decreased diversity among the environments and the general lack of generated variation among the dataset.

The reverse fragments of the representative mice samples yielded an overall negative variation among both IPCA 1 and 2 Figure 11 as evident from the axis total listed previously. The negative values listed by the axis correlated to the difference in sign between the genotype and environment and allowed increased performance in environments having interaction values that were negative. IPCA 1 had more negative variation than IPCA 2. Four of the 6 replicates shared the same data point due to a lack of variation and increased positive interaction amongst those samples. For either sample, all of the replicates were not grouped together. Quadrant 1 contained the most positive correlational replicates and quadrant 3 the most negative. Samples furthest from the origin, L1, had increased sensitivity and adaptive properties and were measured by the relative small length of a projected vector from the origin to the data point. The relatively small sum of squares for the environments of this dataset, which was the smallest measured value of all of the datasets, was due to decreased diversity among the environments and the general lack of generated variation.

Out of the 12 replicates present within the analysis of the forward and reverse fragments in samples H and L, half shared a data point, on the graph (Figure 12). This corresponded to decreased variation and increased interaction amongst those samples as would be evident from a projected vector connecting the data points. The lack of clustering about the origin was representative of increased sensitivity, adaption, and lack of stability to interactions and measured multivariate effects. Of the 12 samples, 10 had at least one positive contributing value from either IPCA 1 or 2. The most positive correlational values in terms of variation were found in Quadrant 1. Quadrant 3 was the most negative. Reverse fragments clustered more amongst each other and away from forward fragments. The relatively small sum of squares from this analysis was comparable to all other datasets.

Margalef diversity index measured species abundance and frequency in all control and symbiotic samples (Figure 13). A larger standard deviation was represented by the relative size of the error bars for the control mice in relation to the synbiotic diet- reflecting a lesser degree of consistency amongst the individual sample replicates. In

contrast, the small standard deviation evident in sample C, a synbiotic diet-fed mouse, reflected replicated results with less variation, and thus the value derived being more representative of the present species richness within the sample. There was a consistency of measured species richness among the control samples as was evident by their relative position on the graph. However, analysis of the data points correlating to the symbiotic diet showed a slight decrease in diversity comparative to the control samples, there was a noticeable spike in the average measured species richness within the synbiotic sample F, and sample L produced the lowest value. Overall trend analysis reflected conservation of species richness during the administration of probiotics.

Therefore, one can conclude that community composition was not inversely disturbed and function and homeostatic balance was maintained as is contrary to antibiotic administration, and there would be a decreased chance of dysbiosis occurring as a side effect to this diet treatment.

Amongst the control samples, B had a greater measured standard deviation than the other two mice which both shared a relatively small error bar size when analyzing the Shannon diversity measure for entropy or abundance of a species amongst a whole community sample (Figure 14). The relatively small standard deviation error bar size of H and J compared to B correlated to a higher degree of representation of the entropy or proportional abundance of a given species amongst a whole as was reflected by this index value. The control diet had the highest degree of variation as sample B also had the highest standard deviation and lowest Shannon diversity index value of all the mice while H yielded the highest Shannon value. The synbiotic mice contained the sample point with the least standard deviation, L. The other mice within this category had the second (F) and third (C) highest standard deviations amongst all of the mice analyzed. The measured Shannon diversity within this category was fairly consistent. When comparing all of the samples together, the measured average Shannon diversity value for the replicates of each sample were similar to one another as differences were based on the hundredth. This supported a conservation of Shannon diversity after then administration of synbiotics when compared to the normal, control diet composition. The consistency across samples alluded to a maintenance and lack of disturbance of gut intestinal community composition and therefore activity upon synbiotic treatment.

When analyzing the Simpson diversity Index (1-λ'), the probability of two randomly selected samples being composed of the same species identification, of both diet categories of cecum content (Figure 15), the control diet contained the top two highest standard deviations (B, J) amongst all of the samples, but it also contained the second smallest measured (H). Mouse H also had the highest diversity value. However, analysis across samples showed a low degree of variation in the average diversity value obtained. Mice fed the synbiotic diet had small standard deviations with the exception of F. The lower standard deviation supported a higher degree of representation to the actual community structure in relation to the species identity measured by this diversity index. The lack of measurable difference in the Simpson values obtained related to a conservation of homeostatic presence and balance after the administration of the synbiotic diet in comparison to the controlled diet concluding to a decreased chance of ensuing dysbiosis from the diet treatment and thus validated the treatment option when compared to the negative effects often resulting from antibiotic or other invasive treatments.

Culture-based techniques have led to novel insights into the study of bacterial community structures of culturable organisms within a given environmental sample. However, there is limited application in revealing the complete diversity or phylogenetic assignment of many of the environments being studied. DNA-based molecular methods facilitate this and circumvent the limited scope of culture dependent techniques by identifying sequence diversity according to genes present within a sample [56]. Species richness is characterized by the number of species within a given community or sample and species evenness refers the size of the species population within that same community. Both are used as parameters to investigate diversity and structure within a community and can be qualitatively estimated based on the unique frequency of occurrence of ribotypes detected during TRFLP. Molecular approaches utilizing isolated total community DNA as a template for study, such as TRFLP which couples PCR and rRNA-based phylogeny, avoid the limitations of cultivation-based studies while providing useful insights into the sample identity by pairing results with database integration [4,34,45,47,48,50-52,54,58,62-64]. Construction, screening, and analysis of clone libraries are both time-and cost-intensive. Other techniques have been developed (such as DNA melting behavior and single-strand conformation) to circumvent clone library use and assess community structure while providing a crude qualitative assessment of species diversity. However, they are limited by the lack of sensitivity of the materials employed in the procedure and do not yield data relative to phylogenetic assignment or identity of a given microbial community. There is also a limitation for presumptive assignment of bacterial group identification within a community [4,45,47,48,54,50-52,58,62,63]. However, the extent of phylogenetic application is dependent of extent of universality and specificity of the primers used. Currently, no known universal primers are present that can hybridize to or amplify all sequences available, and if utilizing cloning for phylogenetic identification, the sequences present in the database used to generate said universal primers represent only a portion of the total species diversity present in the natural microbial world and therefore lack complete resolution [45]. TRFLP analysis therefore stands as a robust, high throughput, automated culture independent means of analysis that bypasses many of the limitations imposed by other techniques employed.

Analysis based on peak area was accomplished due to relative peak height investigation resulting in the presence of the following error: deletion of the smallest peaks, often believed to be within the range of observed noise, causing variation in the level of effect it had on dendogram error rate and thus correlating that those peaks could represent frequently occurring, important TRFs in terms of distinguishing between samples [46]. However, fragment length is not technically representative of an OUT (Operational Taxonomic Unit), as multiple organisms can produce identical TRF profiles [34]. There has also been difficulty reported in designating accurate identity to each TRF in complex community profiles. Each peak in a complex microbial community sample is generally representative of multiple TRFs of the same size produced by multiple taxa [52].

Despite its use and application, interpreting data generated during T-RFLP analysis should be done cautiously and only as an estimation of diversity as population presence is dependent on rank abundance and those microbial populations that are not dominant numerically are often not represented and therefore species diversity of the environmental sample is vastly underestimated. Also, gene

copy number among species and biases introduced though out the procedure can yield skewed, unrepresentative amplicon products in relation to rank abundance of the original DNA sample template. Only very general phylogenetic inferences can be drawn and the degree of phylogenetic information obtainable from this method is dependent on the limited performance of the PCR primer used. Distinct community signatures cannot be produced [4,34,45-48,50-52,54,58,62,63]. Also, the profile reproduction among sample replicates has yet to be achieved in its completeness, thus contributing to a lack of precise community fingerprint and phylogenetic diversity analysis while still providing information pertaining to estimated community richness. Complex community structure has also lead to incongruences between phylotype richness and structure assessment. The inference of phylogenetic composition based on the TRF profile depends on the TRFs phylogenetic resolution (the similarity of organisms responsible for a specific TRF size) and well as the quality and quantity of comparative reference sequences available. Sequence discrimination by a specific TRF is generally inconclusive and generally yields a skew in sequence distribution for a specific TRF, as extremely few TRFs are specific for a given species or genus. Comparative diversity within a community can still be deduced from phylogenetically relevant TRFs. Additionally, there can be discrepancies in fragment sizes due to the relative error apparent from sequence identity on migration within a polyacrylamide gel. This factor can contribute to an alteration in seemingly phylogenetically specific TRFs and the use of 'binning' for comparative TRF sizes.

Various inherent biases are also apparent in relation to applications based on DNA and PCR usage that limit TRF pattern interpretation and relevance though the introduction of error and artifact including those present during sample preparation and DNA isolation, amplification, digestion, electropherogram migration and inconsistencies in gel composition and running conditions, and data set alignment. However, this is not unique to this profiling method but also applies to other microbial community analysis methods currently used [48,52].

Data are presented in this study by means of the AMMI model, which partitions variation measured into main effects and interactions during the analysis of variance through Additive Main Effects and Multiplicative Interactions (ANOVA), and then applies PCA (Principal Component Analysis) to the interactions to create Interaction Principal Components Axis (IPCAs) amongst the samples analyzed allowing for simultaneous visualization of microbial environment and genotype main effects and interactions. PCA allows for a reduction of dimensionality in multivariate data by the creation of key variables that characterize the variation within the complete dataset by serving as a composite of various original variables. The new variables generated do not correlate with one another and are utilized without resulting multicolinearity. TRFLP data was initially analyzed nine different ways according to differing diet and fragment (HEX or FAM) combinations.

In summation the T-RFLP profiles produced had no consistent patterns when analyzing either the forward or the reverse fragments across samples within a given diet or between diets. The shifts in ordinations, applied as the measured distance of projected vectors from the ordinate or from other data points, produced a range of variability, stability, and interaction amongst samples from a given environmental factor (such as diet) as is evident from the data point locations from the origin of the figures previously mentioned. An increased distance from the origin correlated to decreased stability where the means of the measured factors contribute in increased measured variability. Those data points that shared a given quadrant had a positive interaction. The PCA scores or (IPCA%) generated on either axis of the figures represented the interaction intensity of the genotype to the environment; the smaller the score, the less interaction effect, and similarity in sign between these two factors correlated to a positive interaction shown while dissimilarity, the inverse. Stability according to the biplot utilized in this study was more precise than a biplot comprised of only the first PCA axis, though a significant amount of interaction must be contained within the first two axes to be successfully representative. Being relatively high despite ranging among the datasets, a large sum of squares for environments as generally reported in this analysis correlated increased diversity among environments, and the cause of generated variation among the dataset. Variability in both main effects and interactions in relation to environments can be shown by scattered data among environmental locations on a biplot, as was evident in many of the analysis performed, and those high potential environments are evenly distributed in a given quadrant with minimum interaction effect. Lower potential environments clustered in a given quadrant with high IPCA value where lowest yielding environments had the highest positive IPCA scores [54,58].

Qualitative diversity measurements of the TRFLP profiles produced from the cecum content of each of the representative diets generated an overall trend corresponding to conservation of species richness during the administration of probiotics (Figure 13). This supported the conclusion that community composition is not negatively affected, and function and homeostatic balance is maintained, leading to a decreased probability of inducing a diseased state of dysbiosis as a result of probiotic administration which is contrary to the effects of typical antibiotic administration. Also, Shannon diversity values for all samples were comparable due to differences observed according to the hundredth of the value observed (Figure 14). This supported a relative conservation of Shannon diversity between the diets. This consistency also yielded to a preservation and lack of disturbance of gut intestinal community composition and activity upon synbiotic treatment. A reduction in the probability dysbiosis and conservation of homeostatic balance from the diet treatment in addition to validation of the synbiotic treatment option when compared to the negative effects often resulting from antibiotic or other invasive treatments was shown by the lack of significant difference amongst measured Simpson diversity values and low generated standard deviation when compared to the control diet (Figure 15).

Conclusion

These findings supported a higher degree of representation to the actual community structure in relation to the species identity. Further metagenomic studies are necessary to elucidate more exact measures of diversity and phylogenetic assignments for the activity and effectiveness of synbiotics as treatment options to combat dysbiosis and preserve homeostatic balance within the host as is mitigated by the gut microbial flora.

References

1. Paul D Cotter (2011) Small intestine and microbiota. Curr Opin Gastroenterol 27:99-105.
2. Li M, Wang B, Zhang M, Rantalainen M, Wang S, et al. (2008) Symbiotic gut microbes modulate human metabolic phenotypes. Proc Natl Acad Sci USA 105:2117-2122.
3. Saulnier DM, Molenaar D, de Vos WM, Gibson GR, Kolida S (2007) Identification of prebiotic fructooligosaccharide metabolism in Lactobacillus plantarum WCFS1 through microarrays. Appl Environ Microbiol 73:1753-1765.
4. Singh RK, Chang HW, Yan D, Lee KM, Ucmak D, et al. (2017) Influence of diet on the gut microbiome and implications for human health. J Transl Med 15:73.

5. Cunningham-Rundles S, Ahrné S, Johann-Liang R, Abuav R, Dunn-Navarra AM, et al. (2011) Effect of probiotic bacteria on microbial host defense, growth, and immune function in human immunodeficiency virus type-1 infection. Nutrients 3:1042-1070.

6. Curtis TP, Sloan WT (2004) Prokaryotic diversity and its limits: Microbial community structure in nature and implications for microbial ecology. Curr Opin Microbiol 7:221-226.

7. Chen J, He X, Huang J (2014) Diet effects in gut microbiome and obesity. Journal of food science 79:R442-451.

8. Culman SW, Bukowski R, Gauch HG, Cadillo-Quiroz H, Buckley DH (2009) T-REX: software for the processing and analysis of T-RFLP data. BMC Bioinformatics10:171.

9. Culman SW, Gauch HG, Blackwood CB, Thies JE (2008) Analysis of T-RFLP data using analysis of variance and ordination methods: A comparative study. J Microbiol Methods 75:55-63.

10. Rees GN, Baldwin DS, Watson GO, Perryman S, Nielsen DL (2004) Ordination and significance testing of microbial community composition derived from terminal restriction fragment length polymorphisms: Application in multivariate statistics. Antonie van Leeuwenhoek 86:339-347.

11. Blanton C (2014) Personal Communication.

12. Clement BG, Kehl LE, DeBord KL, Kitts CL. (1998) Terminal restriction fragment patterns (TRFPs), a rapid, PCR-based method for the comparison of complex bacterial communities. J Microbiol Methods 31:135-142.

13. Blackwood CB, Marsh T, Kim SH, Paul EA (2003) Terminal restriction fragment length polymorphism data analysis for quantitative comparison of microbial communities. Appl Environ Microbiol 69:926-932.

14. Kostic AD, Howitt MR, W. S. Garrett (2013) Exploring host-microbiota interactions in animal models and humans. Genes Dev 27:701-718.

15. Ley RE, Peterson DA, Gordon JI (2006) Ecological and evolutionary forces shaping microbial diversity in the human intestine. Cell 124:837-848.

16. Liu WT, Marsh TL, Cheng H, Forney LJ (1997) Characterization of microbial diversity by determining terminal restriction fragment length polymorphisms of genes encoding 16S rRNA. Appl Environ Microbiol 63:4516-22.

17. Mazmanian SK, Liu CH, Tzianabos AO, Kasper DL (2005) An immunomodulatory molecule of symbiotic bacteria directs maturation of the host immune system. Cell 122:107-118.

18. Niot I, Poirier H, Tran TT, Besnard P (2009) Intestinal absorption of long-chain fatty acids: Evidence and uncertainties. Prog Lipid Res 48:101-115.

19. Noverr MC, Huffnagle GB (2005) The 'microflora hypothesis' of allergic responses. Clin Exp Allergy 35:1511-1520.

20. O'Hara AM, Shanahan F (2006) The gut flora as a forgotten organ. EMBO Rep 7:688-693.

21. Sadeghi SM, Samizadeh H, Amiri E, Ashouri M (2011) Additive main effects and multiplicative interactions (AMMI) analysis of dry leaf yield in tobacco hybrids across environments. J Biotechnol 10:4358-4364.

22. Zhang X, Zeng B, Liu Z, Liao Z, Li W, et al. (2014) Comparative diversity analysis of gut microbiota in two different human flora-associated mouse strains. Curr Microbiol 69:365-373.

23. Zoetendal EG, Raes J, Van Den Bogert B, Arumugam M, Booijink CC, et al. (2012) The human small intestinal microbiota is driven by rapid uptake and conversion of simple carbohydrates. ISME J 6:1415-1426.

24. Cammarota G, Ianiro G, Bibbo S, Gasbarrini A (2014) Gut microbiota modulation: Probiotics, antibiotics or fecal microbiota transplantation?. IEM 9:365-373.

25. De Wit N, Derrien M, Bosch-Vermeulen H, Oosterink E, Keshtkar S,et al. (2012) Saturated fat stimulates obesity and hepatic steatosis and affects gut microbiota composition by an enhanced overflow of dietary fat to the distal intestine. Am J Physiol Gastrointest 303:G589-99.

26. De Wit NJ, Bosch-Vermeulen H, de Groot PJ, Hooiveld GJ, Bromhaar MM, et al. (2008) The role of the small intestine in the development of dietary fat-induced obesity and insulin resistance in C57BL/6J mice. BMC Med Genomics 1:14.

27. Dethlefsen L, Huse S, Sogin ML, Relman DA (2008) The pervasive effects of an antibiotic on the human gut microbiota, as revealed by deep 16S rRNA sequencing. PLoS Biol 6:e280.

28. Dethlefsen L, McFall-Ngai M, Relman DA (2007) An ecological and evolutionary perspective on human–microbe mutualism and disease. Nature 449:811-818.

29. Stefano Di Bella, Cecilia Drapeau, Esther García-Almodóvar, Nicola Petrosillo (2013) Fecal microbiota transplantation: the state of the art. Curr Infect Dis Rep 5:13.

30. Druart C, Neyrinck AM, Dewulf EM, De Backer FC, Possemiers S, et al . (2013) Implication of fermentable carbohydrates targeting the gut microbiota on conjugated linoleic acid production in high-fat-fed mice. Br J Nutr 110:998-1011.

31. Druart C, Neyrinck AM, Vlaeminck B, Fievez V, Cani PD, et al. (2014) Role of the lower and upper intestine in the production and absorption of gut microbiota-derived PUFA metabolites. PloS One 9:e87560.

32. Dunbar J, Ticknor LO, Kuske CR (2001) Phylogenetic specificity and reproducibility and new method for analysis of terminal restriction fragment profiles of 16S rRNA genes from bacterial communities. Appl Environ Microbiol 67:190-197.

33. Langille MG, Meehan CJ, Koenig JE, Dhanani AS, Rose RA, et al. (2014) Microbial shifts in the aging mouse gut. Microbiome 2:50.

34. O'Shea EF, Cotter PD, Stanton C, Ross RP, Hill C (2012) Production of bioactive substances by intestinal bacteria as a basis for explaining probiotic mechanisms: Bacteriocins and conjugated linoleic acid. Int J Food Microbiol 152:189-205.

35. Blaser M.J (2019) Fecal microbiota transplantation for dysbiosis-predictable risks. N Engl J Med 381: 2065-2066.

36. Caporaso JG, Lauber CL, Walters WA, Berg-Lyons D, Lozupone CA, et al. (2011) Global patterns of 16S rRNA diversity at a depth of millions of sequences per sample. Proc Natl Acad Sci 108:4516-4522.

37. Nicholson JK, Holmes E, Wilson ID (2005) Gut microorganisms, mammalian metabolism and personalized health care. Nat Rev Microbiol 3:431-438.

38. Fritz JV, Desai MS, Shah P, Schneider JG, Wilmes P (2013) From meta-omics to causality: Experimental models for human microbiome research. Microbiome 1:14.

39. Hayashi H, Takahashi R, Nishi T, Sakamoto M, Y. Benno (2005) Molecular analysis of jejunal, ileal, caecal and recto-sigmoidal human colonic microbiota using 16S rRNA gene libraries and terminal restriction fragment length polymorphism. J Med Microbiol 54:1093-1101.

40. Osborn AM, Moore ERB, Timmis KN (2000) An evaluation of terminal restriction fragment length polymorphism (T-RFLP) analysis for the study of microbial community structure and dynamics. Environ Microbiol 2:39-50.

41. Linninge C, Xu J, Bahl MI, Ahrné S, Molin G (2019) Lactobacillus fermentum and Lactobacillus plantarum increased gut microbiota diversity and functionality, and mitigated Enterobacteriaceae, in a mouse model. Beneficial microbes 10:413-424.

42. Borody TJ, Khoruts A (2012) Fecal microbiota transplantation and emerging applications. Nat Rev Gastroenterol Hepatol 9:88-96.

43. Froebel LK, Jalukar S, Lavergne TA, Lee JT, Duong T (2019) Administration of dietary prebiotics improves growth performance and reduces pathogen colonization in broiler chickens. Poult Sci 98:6668-6676.

44. Hooper LV (2004) Bacterial contributions to mammalian gut development. Trends Microbiol 12:129-134.

45. Lazarevic V, Whiteson K, Huse S, Hernandez D, Farinelli L, et al. (2009) Metagenomic study of the oral microbiota by Illumina high-throughput sequencing. J Microbiol Methods 79:266-271.

46. Sartor RB (2008) Microbial influences in inflammatory bowel diseases. Gastroenterlogy 134:577-594.

47. Siqueira JF, Sakamoto M, Rosado AS. Microbial community profiling using terminal restriction fragment length polymorphism (T-RFLP) and denaturing gradient gel electrophoresis (DGGE). InOral Biology 2017 (pp. 139-152). Humana Press, New York, NY.

48. Walsh CJ, Guinane CM, O'Toole PW, Cotter PD (2014) Beneficial modulation of the gut microbiota. FEBS Lett 588:4120-4130.

49. Magrone T, Jirillo E (2013) The interaction between gut microbiota and age-related changes in immune function and inflammation. Immun Ageing 10:31.

50. Ley RE, Bäckhed F, Turnbaugh P, Lozupone CA, Knight RD, et al. (2005) Obesity alters gut microbial ecology. Proc Natl Acad Sci U S A 102:11070-11075.

51. Schütte UME, Abdo Z, Bent SJ, Shyu C, Williams CJ, et al. (2008) Advances in the use of terminal restriction fragment length polymorphism (T-RFLP) analysis of 16S rRNA genes to characterize microbial communities. Appl Microbiol Biotechnol 80:365-380.

52. Stres B (2006) The first decade of terminal restriction fragment length polymorphism (T-RFLP) in microbial ecology. Acta agriculturae Slovenica 8:65œ73.

53. Hilton A, Armstrong RA (2006) Statnote 6: One-way analysis of variance (ANOVA). Microbiologist 33-37.

54. Konstantinidis KT, Tiedje JM (2005) Genomic insights that advance the species definition for prokaryotes. Proc Natl Acad Sci USA. 102:2567-2572.

55. Costello EK, Lauber CL, Hamady M, Fierer N, Gordon JI, et al. (2009) Bacterial community variation in human body habitats across space and time. Science 326:1694-1697.

56. Rankoff-Nahoum S, Paglino J, Eslami-Varzaneh F, Edberg S, Medzhitov R (2004) Recognition of commensal microflora by toll-like receptors is required for intestinal homeostasis. Cell 118:229-241.

57. Bäckhed F, Ding H, Wang T, Hooper LV, Koh GY, et al. (2004) The gut microbiota as an environmental factor that regulates fat storage. Proc Natl Acad Sci 101:15718-15723.

58. McGarr SE, Ridlon JM, Hylemon PB (2005) Diet, anaerobic bacterial metabolism, and colon cancer: A review of the literature. J Clin Gastroenterol 39:98-109.

59. Saulnier DM, Ringel Y, Heyman MB, Foster JA, Bercik P, et al. (2013) The intestinal microbiome, probiotics and prebiotics in neurogastroenterology. Gut Microbes 1:17-27.

60. Abdo Z, Schüette UM, Bent SJ, Williams CJ, Forney LJ, et al. (2006) Statistical methods for characterizing diversity of microbial communities by analysis of terminal restriction fragment length polymorphisms of 16S rRNA genes. Environ Microbiol 8:929-938.

61. Raju BMK (2002) A study on AMMI model and its biplots. J Indian Soc Agric Stat 55:297-322.

62. Khoruts A, Dicksved J, Jansson JK, Sadowsky MJ (2010) Changes in the composition of the human fecal microbiome after bacteriotherapy for recurrent Clostridium difficile-associated diarrhea. J Clin Gastroenterol 44:354-360.

63. Klemashevich C, Wu C, Howsmon D, Alaniz RC, Lee K, et al. (2014) Rational identification of diet-derived postbiotics for improving intestinal microbiota function. Curr Opin Biotechnol 26:85-90.

64. Mujico JR, Baccan GC, Gheorghe A, Díaz LE, Marcos A (2013) Changes in gut microbiota due to supplemented fatty acids in diet-induced obese mice. Br J Nutr 110:711-720.